Desalination and Water Treatment
www.deswater.com

doi: 10.5004/dwt.2022.27942

245 (2022) 72–84
January

Techno-economic assessment of carbon-based nanofluid dispersions in solar stills for rural coastal locations in the Northern and Southern hemispheres

Sai Kiran Hota[a], Carlos Mata-Torres[b], Jose Miguel Cardemil[c], Gerardo Diaz[d,*]

[a]*Advanced Cooling Technologies, 1046 New Holland Avenue, Lancaster, PA, 17601, USA, email: saikiran.hota@1-act.com*
[b]*Pacific Green Solar Technologies, PGTK Group, Madrid, Spain, email: cnmata@uc.cl*
[c]*Pontificia Universidad Católica de Chile, Avda. Vicun˜a Mackenna 4860, Macul, Santiago, Chile, email: jmcardem@uc.cl*
[d]*Department of Mechanical Engineering, University of California, 5200 North Lake Rd., Merced, CA, 95343, US, email: gdiaz@ucmerced.edu*

Received 9 July 2021; Accepted 25 October 2021

ABSTRACT

Accessibility of freshwater in remote rural regions where the demand is merely of the order of 1 to 100 m^3/d is limited. Low-cost freshwater productivity in those regions can be fulfilled by simple solar stills with inexpensive carbon particle dispersions to enhance the absorption of solar energy near the evaporating surface. In this manuscript, the techno-economic and environmental assessment of such a solar still with low-cost nanoparticle dispersion is performed for two rural coastal locations of Big Sur (U.S.A) in northern hemisphere and Chañaral (Chile) in southern hemisphere and compared against competing solar desalination technologies, that is, solar collector integrated humidification dehumidification (FPC- HDH) and photo-voltaic seawater reverse osmosis (PV-SWRO) system. Real time year-round solar irradiation and ambient conditions data are utilized for the energy analysis. The expected daily freshwater productivity is around 3.5 and 5 m^3/d for a 1000 m^2 solar still and FPC-HDH system. For similar rates of freshwater productivity, 200 m^2 PV-SWRO system is sufficient. The annual greenhouse gas emissions mitigated by thermal systems was around 200 ton/y, while for PV-SWRO was only 50 ton/d. Economic analysis showed cost of freshwater production with solar still to be lower than PV-SWRO at around \$8/m^3. A feasibility analysis of low-cost parameters showed that the unit cost of freshwater can be lower than \$3/m^3 with solar stills, which is much lower than PV-SWRO system.

Keywords: Carbon-based dispersions; Solar stills; Levelized cost of water (LCOW)

1. Introduction

Freshwater demand continues to increase steadily with population growth, while availability of freshwater sources is becoming scarcer. Desalination systems that process seawater (or brackish water) are currently being developed with emphasis on sustainable energy sources, such as solar energy. For large volumes of daily freshwater requirements, that is, of the order of a million of liters per day, photo-voltaic reverse osmosis of seawater (PV-SWRO), solar thermal/geothermal based multi-stage flash (MSF), and multi-effect distillation (MED) are prevalent [1]. These large volumes of freshwater production are suitable for urban regions and locations in their vicinity. However, in many regions of the world, around 50% of the remote rural areas have little to no access to freshwater [2]. The daily freshwater demand in these regions is much lower than in urban regions, so adopting the above-mentioned systems might not be feasible considering the cost of freshwater production.

* Corresponding author.

For low volumes of freshwater production, direct solar desalination systems such as solar stills and humidification dehumidification (HDH) systems can be utilized. It is noted in the literature that, for daily freshwater requirement of less than 200 m^3/d, solar stills are more favorable over other desalination technologies [3]. Likewise, in recent years, HDH systems have gained attention for low-volume production. Advances in PV and RO technologies have also made PV-RO systems more feasible for low-volume production. Some typical costs of freshwater production ($/$m^3$) utilizing these technologies are shown in Table 1.

Typical costs of freshwater from the literature for low-volume productivity range from 3 to 40 $/$m^3$. In this analysis, a comparative assessment of solar stills, PV-SWRO and flat plate collector (FPC) integrated HDH (FPC-HDH) systems for two rural locations in the northern hemisphere (Big Sur, U.S.A) and southern hemisphere (Chañaral, Chile) is performed. These two regions were selected as regions with high solar irradiance and thus suitable for solar-powered desalination. In this manuscript, emphasis is placed on assessing the competitiveness of solar still in comparison to FPC-HDH and PV-SWRO. The inherent advantage of solar stills over other technologies is that it is passive in construction and the operation is relatively simple. Recently, it was noted that the cost of water produced by a solar still made of fiber reinforced plastic (expensive material) could be only INR 1.32/L ($17.6/$m^3$) and is closer to that of an RO system at INR 1/L ($13.3/$m^3$) [1 USD ≈ 75 INR] [10]. A solar still designed to meet 300 l/d freshwater requirement could produce water costing between 6.3 and 8.2 $/$m^3$ [11]. In solar stills, nanoparticle dispersions can be used effectively for productivity enhancement. Arunkumar et al., [12] reviewed various metallic nanofluids and multi-walled carbon-nanotube based nanofluids used in solar still productivity enhancement. The advantage of having these particles is that they convert the incident solar energy into heat near the evaporating surface. As a result, the surface temperature increases, enhancing the evaporation rate of water in addition to keeping the bulk volume near ambient temperature. Black painted solar still basins on the other hand augment energy losses because they heat up the entire volume of water, losing energy from the bottom and sides of the solar still [13]. Low-cost carbon-based particles such as biochar and activated carbon offer an economical advantage along with productivity improvement over metallic nanoparticles [13,14]. Several researchers have utilized different forms of carbon as small particle dispersions in solar stills [15–17]. They noted that the freshwater productivity rate increases by almost 30% to 40%. Low-cost small particles like biochar can be used for solar absorption with little to no change in capital cost of the solar still system. Also, it is expected that these particles can be washed and reused, so replacement costs are reasonable.

Based on the technical literature, there still a large potential for improvements in solar stills, especially regarding the increase in productivity, when combined with the use of nanoparticles. In that context, the present article describes a detailed assessment of an enhanced solar still, based on a validated thermodynamic methodology. The analysis carried out constitutes a new approach which allows to evaluate the impact of using low-cost carbon-based nanoparticles in solar stills, assessing the impact of its concentration, and analyzing the effects of increasing the scale of the system. Thus, the analysis, allows also to assess the competitiveness of solar stills, compared to other desalination technologies commonly employed for small communities.

The organization of the manuscript is as follows: in Section 2, the system description and the methodology are explained. Section 3 describes the energy analysis for freshwater productivity rate, the annual greenhouse gas emission mitigation rate from these systems, and the method for evaluating the cost of freshwater. In section 4, the system performance characterization at 1 sun, the estimated daily freshwater productivity rate for 1 y in both locations, and the corresponding greenhouse gas emissions mitigation and cost of freshwater produced are presented and explained.

2. Methodology

The system configuration for the three chosen desalination technologies is shown in Fig. 1. A solar still basin area of 1,000 m^2 was selected considering a minimum of 1 L/m^2 d freshwater productivity rate in winter conditions. Likewise, for the FPC-HDH system, a solar collector area of 1,000 m^2 was selected for uniformity.

As shown in Fig. 1, a single-slope single-basin solar still is considered due to its simplicity in construction. In the case of the FPC-HDH system, a closed-air open-water configuration was selected. The maximum seawater temperature is limited to 90°C as it is close to the boiling point, but it limits scale formation on the system.

Additional usable thermal energy is assumed to be stored in a thermal energy storage (TES) unit. This additional energy is later used to desalinate more seawater during the evening hours. The electrical energy produced from the PV system increases the pressure of seawater on

Table 1
Reported unit cost of water

Technology	Energy source	Capacity (m^3/y)	Cost of water ($/$m^3$)
HDH [4]	Heat pump	–	6–7.14
HDH [5]	Solar collector	16.43–19.45	32–38
SWRO [6]	PV	3	16.27
SWRO [7]	PV	<100	3–35.9
Solar still [8]	Solar still	1	16.3
Solar still [9]	Solar still	50	2.4

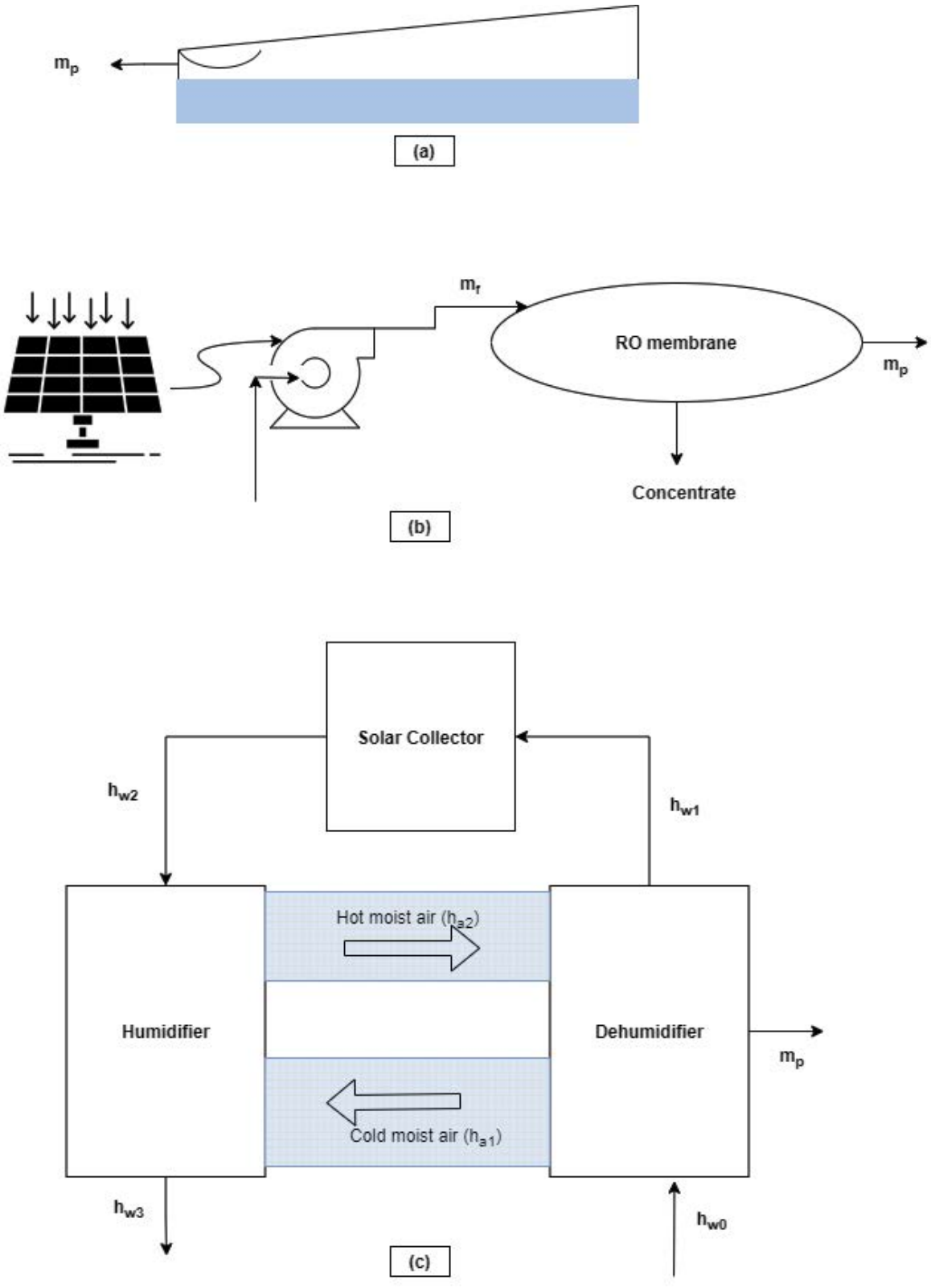

Fig. 1. Selected configuration for (a) Solar still, (b) PV-SWRO, and (c) FPC-HDH desalination systems.

the SWRO membranes. The maximum feed pressure on the membranes is limited to 55 bar. Similar to the FPC-HDH unit, additional usable electrical energy is stored in a battery storage unit and this is discharged at various intervals to produce more freshwater from the SWRO unit.

3. Energy and economic analysis

3.1. Energy analysis

The mass and energy balances for the desalination process that allow computing the freshwater production are described in Table 2. Saline (sea) water with 3.5% salt concentration is assumed to enter these units at ambient temperature. The notation used for the energy balance of the HDH system follows the terminology used in [18].

Likewise, the parameters used for the RO governing equations follow the definitions stated in [19–21]. The overall computations were carried out by making use of the governing equations outlined in Table 2 subject to the following assumptions:

3.1.1. Solar still [22]

- The heat capacity of the glass, basin, and the insulation are neglected and the heat losses from the glass walls are considered negligible.
- The solar still is vapor/air leakage proof.
- The temperature of the water mass is considered uniform with no stratification.

3.1.2. HDH unit [18]

- The HDH unit operates at steady state and heat losses to the ambient are neglected.
- The fan/blower power is negligible in comparison to the output from solar water collector [18,23].
- The thermal and hydraulic losses between collector and the HDH unit are ignored.

3.1.3. RO unit [24]

- The liquid water is considered to be incompressible with known temperature and pressure conditions.
- The permeate flows at ambient pressure conditions (P_{atm} = 1 bar).
- The fouling factor varies with time as mentioned in [21].

Small carbon particle dispersions increase solar absorption near the evaporating surface of water in a solar still. The intensity of absorption increases with increasing volume fraction of the particles until an optimum (f_v) is reached [25,26]. The solar absorption in water is quantified as the fluid absorption (α_w).

The governing equations for the solar still described in Table 2 result in a transient ordinary differential equation, which has a solution of the form:

$$T_w = \frac{\bar{f}(t)}{a}\left(1-\exp(-at)+T_{w0}\exp(-at)\right) \tag{1}$$

where T_w is the water mass temperature, $\bar{f}$ is a function of effective light absorptance and heat loss coefficient, T_{w0} is the initial water mass temperature, a represents thermal time constant, and t is computational time, which is 1 h. These terms are described in depth in [22,27].

The solar collectors are modeled according to the thermal energy balance outlined in [28,29], and the PV modules are modeled according to [30–32].

The top heat loss from the transmitting glass to the ambient consists of convection and radiation losses given as:

$$h_{tga} = h_{cba} + h_{rga} \tag{2a}$$

$$h_{cba} = 2.8 + 3u \tag{2b}$$

$$h_{rga} = \epsilon_g\,\sigma\left(T_g^2 + T_{sky}^2\right)\left(T_g + T_{sky}\right) \tag{2c}$$

where T_g and T_{sky} are the glass and sky temperatures, respectively. The bottom heat loss coefficient from the body to the ambient is given as [33]

$$h_{ba} = 5.7 + 3u \tag{3}$$

Some thermo-physical and optical properties are considered as constants for the computations. Those properties are summarized in Table 3.

The energy consumed to produce 1 m^3 of freshwater by these processes is called specific energy consumption (SEC). The greenhouse gas emissions mitigated annually are then calculated considering an emission factor of 0.231 kg CO_2/kWh of energy consumed assuming that natural gas burned at a power plant is substituted by the solar systems at a thermal and electrical conversion factor of 80% and 45%, respectively [38].

For the economic analysis, the levelized cost of water (LCOW) method is adopted which is calculated as [39]:

$$\text{LCOW} = \frac{\text{CAPEX} + (\text{OPEX})\text{PVF}(d,n)}{(\text{Annual Productivity})\text{PVF}(d,n)} \tag{4}$$

Carbon credits, salvage (residual) value, annual asset depreciation, and annual energy metering adjustments are some of the items that fall under the category of adjustments. CAPEX and OPEX are the total capital cost ($) and the annual operational cost of the system ($/y), respectively. Present value of running costs is normalized by the present value function (PVF) for discount rate d and a project life (n) of 25 y, given as:

$$\text{PVF}(d,n) = \frac{(1+d)^n - 1}{d(1+d)^n} \tag{5}$$

The cost of the solar collector field can be divided into area-dependent and area independent costs. The area-independent cost is a fixed value that considers items such as piping connections, pump, electrical wiring, and other ancillary components.

This fixed cost was considered to be of $50,000 for the selected solar area [40]. The solar collector cost was considered at $350/m^2 based on the applicable correlations [41,42], while the cost of thermal energy storage was considered to be $20/kWh.

Table 2
Energy and mass balancing of desalination systems

Technology	Governing equations	Performance metrics
Solar Still [22,27]	Glass cover: $\alpha_g' I + h_{\text{twg}}\left(T_w - T_g\right) = h_{\text{tga}}\left(T_g - T_{\text{amb}}\right)$	$h_{\text{cwg}} = 0.884\left[\left(T_w - T_g\right) + \frac{\left(\left(P_w - P_g\right)T_w\left(K\right)\right)}{268900 - P_w}\right]^{\frac{1}{3}}$
	Water mass: $m_w C_{\text{pw}} \frac{dT_w}{dt} = \alpha_w' I + h_{\text{twg}}\left(T_g - T_w\right) + h_{\text{cbw}}\left(T_b - T_w\right)$	$h_{\text{ewg}} = 0.0163\frac{h_{\text{ewg}}\left(P_w - P_g\right)}{T_w - T_g}$
	Basin: $\alpha_b' I = h_{\text{cbw}}\left(T_b - T_w\right) + h_{\text{cba}}\left(T_b - T_{\text{amb}}\right)$	$h_{\text{rwg}} = \in_{\text{wg}} \sigma\left(T_w^2 + T_g^2\right)\left(T_w - T_g\right)$
	$h_{\text{twg}} = h_{\text{cwg}} + h_{\text{ewg}} + h_{\text{rwg}}$	$m_{\text{hour}} = \frac{Q_{\text{ewg}}}{I(t)A} 3{,}600\left(\text{kg/h}\right)$
	$Q_{\text{ewg}} = h_{\text{ewg}} A\left(T_w - T_g\right)$	$\eta_{\text{still}} = \frac{Q_{\text{ewg}}}{IA}$
HDH [18,23]	Dehumidifier mass balance: $m_{da}\left(\omega_{a2} - \omega_{a1}\right) = m_p\left(\text{kg/s}\right)$	$h_a = h_{\text{da}} + \omega h_w$
		$Q_{htf} = m_w\left(h_{w2} - h_{w1}\right)$
	Humidifier mass balance: $m_w = m_p + m_b$	$\in_{dh} = \max\left(\frac{H_{a2} - H_{a1}}{H_{a2} - H_{a,\text{ideal}}}, \frac{H_{w0} - H_{w1}}{H_{w0} - H_{w,\text{ideal}}}\right)$
	Dehumidifier energy balance: $m_{da}\left(h_{a2} - h_{a1}\right) = m_p h_p + m_w\left(h_{w1} - h_{w0}\right)$	$\in_h = \max\left(\frac{H_{a1} - H_{a2}}{H_{a1} - H_{a,\text{ideal}}}, \frac{H_{w2} - H_{w3}}{H_{w2} - H_{w,\text{ideal}}}\right)$
	Humidifier energy balance: $m_{\text{da}}\left(h_{a2} - h_{a1}\right) = m_w h_{w2} - m_b h_{w3}$	$m_{\text{hour}} = m_p \times 3{,}600\left(\text{kg/h}\right)$
RO [19,34]	Permeate flow: $m_p = \left(A_w \text{TCF FF}\right) S_e\left(\Delta\bar{P} - \Delta\bar{\pi}\right)\left(kg/s\right)$	$m_{\text{hour}} = m_p \times 3{,}600\left(\text{kg/h}\right)$
		$X_p < 0.5\left(\text{g/kg}\right)$
	Salt flow: $X_p = \left(\left(B_w \text{TCF}\right) S_e \text{CPF}\left(\Delta X - X_p\right)\right) / m_p$	
	Water mass balance: $m_w = m_p + m_b$	
	Concentration balance: $m_w X_w = m_p X_p + m_b X_b$	

Similarly, a PV module price of 2.25 $/W [43] was selected for 220 kW_p PV plant. The cost of the high pressure pump (HPP) can be approximated by the correlation [44] HPP = 52($Q_{\text{fh}}P_f$), where Q_{fh} is the hourly feed flow rate, in m^3/h, and P_f is the feed pressure, in bar. The capital cost of battery storage is taken as $300/kWh with the cost of components being $387/kW [45]. The solar still on the other hand, is assumed to be made of long lasting inexpensive materials. A simple calculation of 1 m^2 solar still made of concrete leveling and stainless steel basin had a capital cost of $46/$m^2$ excluding sealants, iron brackets and pumping, with material price estimates from [46]. For the present analysis, the capital cost for the solar still was considered to be $80/$m^2$, which corresponds to a conservative estimate. It was considered that the indirect costs associated were 10% of direct capital for contingency and 5% of direct capital cost for freight and insurance [47]. Annual operation and maintenance cost were considered to be 1.5% of total capital cost excluding annualized replacement of parts, which were estimated to be 10% for the thermal energy storage (TES), 10% for the high pressure pump and 20% for RO membranes. Labor costs differed between the regions due to differences in hourly wages. The annual labor for Big Sur was considered as $25,000, while that for Chañaral was $15,000. The labor costs for solar stills are significantly lower than these two complex technologies, and was estimated to be about $0.1–0.5

Table 3
Thermophysical and optical constants

Solar Still	solar collector – HDH	PV-RO
Glass properties	Glass properties	Glass properties
$\alpha_g = 0.05$	$\alpha_g = 0.05$	$\alpha_g = 0.05$
$\rho_g = 0.9$	$\rho_g = 0.9$	$\rho_g = 0.9$
Water properties	Absorber properties	PV properties
$R_w = 0.05$	$\alpha_{abs} = 0.95$	$\alpha_{pv} = 1$
$\rho_w = 0.96$	HDH effectiveness	$\beta_{pv} = 0.00468$ [36]
Basin properties: non selective	$\varepsilon_h = \varepsilon_{dh} = 0.92$ [18]	Backsheet properties
$\alpha_b = 0.6$	$T_p = f(T_{da1}, T_{da2})$ [35]	$\rho_b = 0.85$
$R_b = 0.3$	$Tw0 = T$amb	A_w and B_s for SW30HR-380 [37]

[48]. In this analysis, it is estimated to be around \$5/m^2. Carbon credits are not applied, although, these installations can avail them at around \$15/ton of CO_2 emissions abated.

4. Results and discussions

4.1. Solar thermal system and desalination characterization

The efficiency curve of the solar thermal systems is characterized under the standard radiation of 1 sun (1 kW/m^2), assuming normal ambient conditions as 27°C and 1 m/s wind velocity. A saline feed flow rate of 1 kg/s is utilized for this analysis, with the objective of understanding the operating characteristics and scaling effects of the solar and desalination systems.

The efficiency curves for these systems are shown in Fig. 2a, where it is observed that the efficiency of solar collectors deteriorates at higher reduced temperatures [28,49], while the solar still efficiency curve, on the other hand, increases with the evaporation temperature due to increasing mass fraction gradient between evaporating and condensing surfaces [25]. Fig. 2a shows the solar still efficiency curves for two conditions, at absorptance-transmittance product ($\alpha\tau$) of 0.59 (non-black condition) and 0.89 (dispersion/bottom black condition). It is observed that higher values of ($\alpha\tau$) develop significantly higher solar still efficiencies.

$$\left(T^* = \frac{T - T_{amb}}{I}\right) \tag{6}$$

Fig. 2b shows the variation of the freshwater productivity with solar collection area. It is assumed that the evaporation flux in a solar still remains constant and thereby increasing the basin area linearly increases total distillate production. In the case of the FPC-HDH system, a detectable productivity is observed at around 40 m^2 of total area, and at about 80 m^2, it presents similar distillate production rate as the high-absorption solar still. The PV-SWRO system on the other hand, requires a minimum PV area of 20 m^2 for desalination. The reason being, a minimum threshold pressure of 40 bar is needed to obtain fresh water with acceptable permeate quality. Further increasing the solar area raises the feed pressure thereby increasing the permeate production, until a maximum allowable feed pressure is achieved.

4.2. Influence of black particle dispersions

Higher transmittance-absorptance product in solar stills depends on the dispersion attenuation strength and number concentration. The dispersion concentration increases the solar absorption fraction within the fluid itself until an optimum level of concentration is reached [25]. The advantage of having particle dispersions over a solar still with the bottom surface painted black is that, with dispersions, the light from the sun is absorbed near the surface of the water, increasing its temperature near this region, thereby enhancing the evaporation rate. Since most of the light is absorbed near the surface of the water, there is no need to include a bottom surface painted black. On the other hand, for the black basin, higher water-surface temperatures are possible only after the entire fluid volume has been heated. Also, a poorly insulated system loses heat from the bottom of the basin almost instantaneously, whereas, due to localized heating in particle dispersions, the bulk fluid volume remains at a low temperature [25]. Nanoparticles can be easily dispersed by ultrasonic dispersion before introducing into the solar still [16]. Since the suspensions are stable, resuspension can be achieved by introducing makeup water in a weekly manner.

Fig. 3 shows the increase in the solar absorption coefficient for a solution with dispersed black particles (e.g., activated carbon of 8μm in size) with respect to volume concentration, where the maximum annual productivity is achieved between 0.05 and 0.1% volume concentration. Low-cost black carbon particles like activated carbon and biochar were found to have zeta potential lower than –40 mV [26,13]. According to the literature, if zeta potential is greater than ±|20| mV, the nanofluid is stable [50]. Since the maximum required particle dispersion is below 0.1%, it can be computed from [51] where the properties of base fluid (water) are relatively unaffected. Outdoor experiments have shown up to 100% water evaporation enhancement by using activated carbon particle dispersions at 0.1% concentration [26]. As shown in [25], the cost effective micron-size particles at a slightly higher concentrations are as effective for strong solar absorption as expensive nanoparticles. From the curves depicted in Fig. 3, it is observed that the solar absorption fraction and the annual distillate productivity have a similar behavior with respect to volume fraction. The annual productivity of a

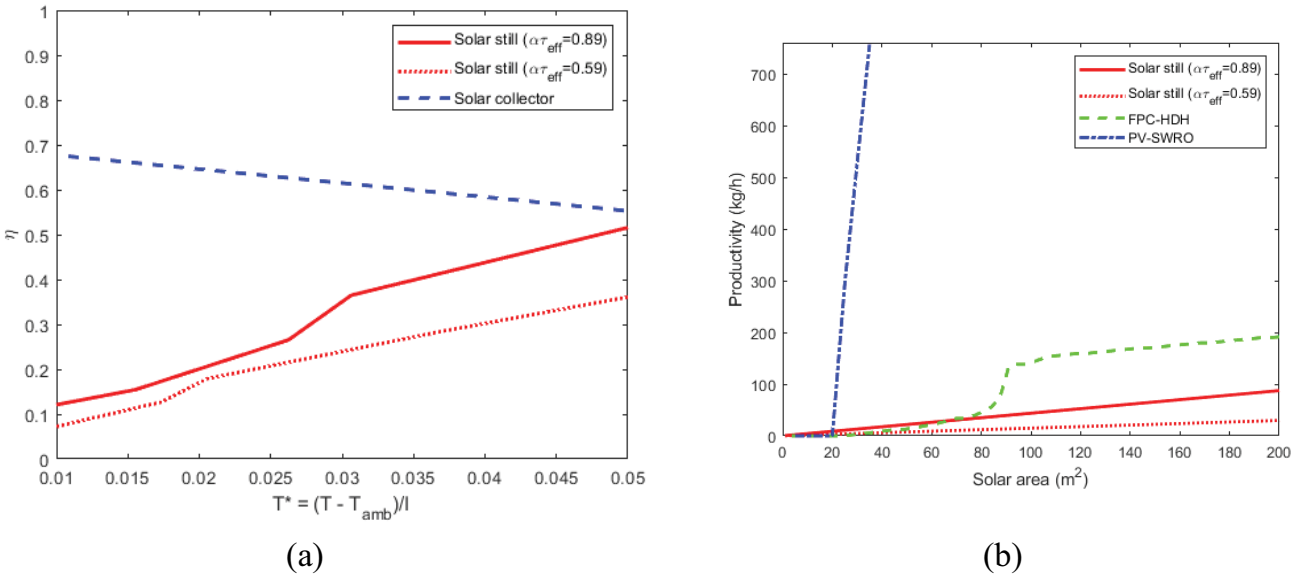

Fig. 2. (a) Efficiency of solar units and (b) hourly productivity of solar still in com- parison to FPC-HDH system and PV-SWRO.

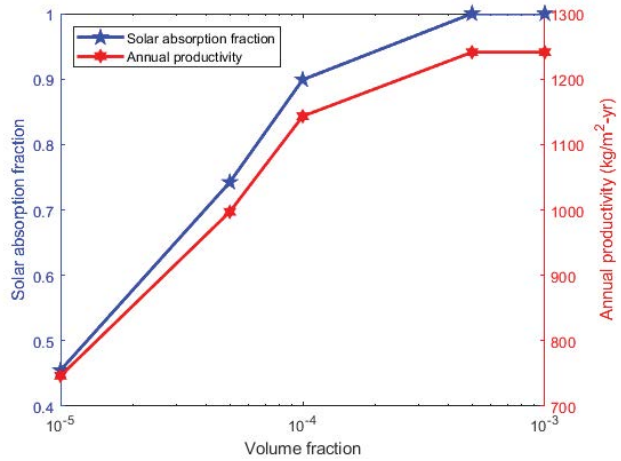

Fig. 3. Influence of particle dispersion volume fraction in distillate productivity.

conventional solar still without any particle dispersion was estimated as 743.07 kg/m^2-y, while that for 0.1% volume concentration, was 1,241 kg/m^2-y (TMY data corresponds to location of Big Sur).

Therefore, introducing strong solar absorbing particles translates into a distillate productivity enhancement of 67%. Sharshir et al. [15] noted that the productivity with 1.2–1.3 μm size graphite particles increased by 45%. For the analysis described in the following sections, it is assumed that the fluid solar absorption fraction is equal to one, with appropriate particle concentration.

4.3. Year-round freshwater production

Solar radiation and weather data for two coastal locations are considered for Big Sur in U.S.A (northern hemisphere) and Chañaral in Chile (southern hemisphere). The meteorological data was assembled in a TMY file format, which is shown in Fig. 4.

The freshwater productivity curves for the three desalination technologies follow the incident solar radiation. Mean winter productivity for PV-SWRO is higher compared to both, solar stills and FPC-HDH, while for summer conditions, average productivity of FPC-HDH is comparatively higher than the other two desalination systems. Summer productivity for the solar stills is roughly between 5.2 and 5.5 m^3/d, while that for the FPC-HDH is 7.2–8.02 m^3/d. The annual average calculated for these three desalination technologies, along with conventional solar still (CSS) with no particles, for 96% plant availability is shown in Table 4.

Surplus energy is accumulated in both FPC-HDH and PV-SWRO systems due to the maximum temperature and maximum pressure on RO membrane, respectively. Monthly accumulated thermal and electrical energy are shown in Fig. 5.

It is observed from Figs. 5a and b that excess thermal energy is available during part of spring and during the complete summer, while, during fall and winter conditions, the solar collectors use all the incident solar irradiation to heat the saline water fed to the system. For PV-SWRO, the excess electrical energy is available all over the year. Freshwater production by using this TES discharged thermal energy on average was found to be 52.02 m^3/y (3.2% of total distillate) in Big Sur, and 155.48 m^3/y (8.48% of total distillate) in Chañaral. In the case of PV-SWRO, additional freshwater productivity by utilizing this energy at 90% battery efficiency is 800.73 m^3/y in Big Sur, and 883.91 m^3/y in Chañaral. The total annual freshwater productivity with PV-SWRO including batteries is then 1,815.24 m^3/y (5.19 m^3/d) in Big Sur, and 2,090.32 m^3/y (5.97 m^3/d) in Chañaral, respectively. The freshwater productivity rate with PV-SWRO system incorporating a battery energy storage for more desalination is higher than the other two thermal desalination systems.

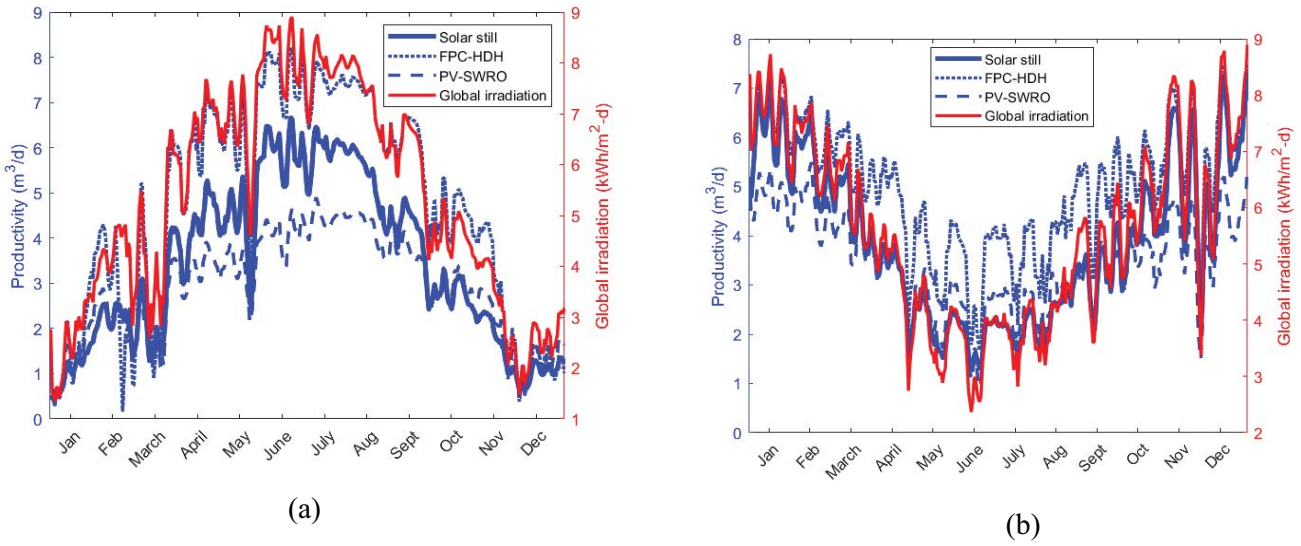

Fig. 4. Year round fresh water productivity in (a) Big Sur and (b) Chañaral.

Table 4
Average annual productivity

Location	Solar still (m^3/d)	CSS (m^3/d)	FPC-HDH (m^3/d)	PV-SWRO (m^3/d)
Big Sur (U.S.A)	3.415	2.13	4.79	2.89
Chañaral (Chile)	3.849	2.38	5.24	3.45

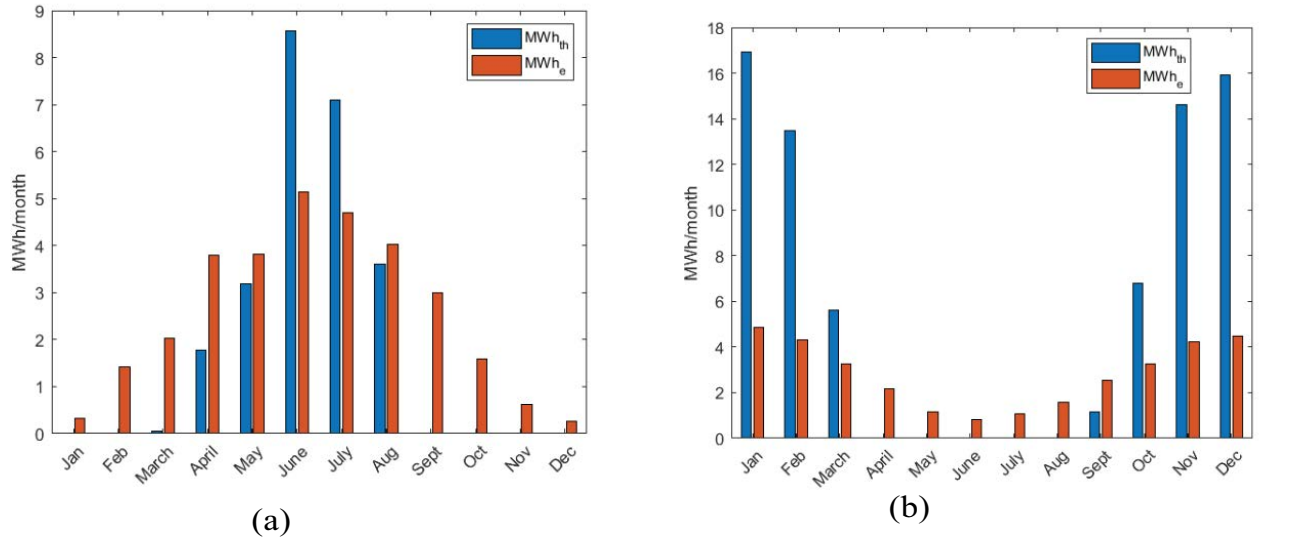

Fig. 5. Surplus of thermal and electrical energy (a) Big Sur and (b) Chañaral.

4.4. Greenhouse gas emissions reduction

Specific energy consumption (SEC) depends on the incident irradiation and the fresh-water productivity for a given day. A simple single stage evaporating unit consumes between 650 to 800 kWh of thermal energy for desalinating 1 m^3 of water [38], while that of PV-SWRO is significantly lower than that of a thermal system.

Figs. 6a–f show specific energy consumption (SEC) for producing fresh water and total CO_2-eq emissions mitigated. In solar stills and FPC-HDH, the SEC is typically around 500 to 600 kWh/m^3, while SEC for PV-SWRO is around 50 kWh/m^3. However, it is not feasible to use FPC-HDH for productivities lower than 3 m^3/d due to its high SEC. The corresponding emissions mitigated show almost

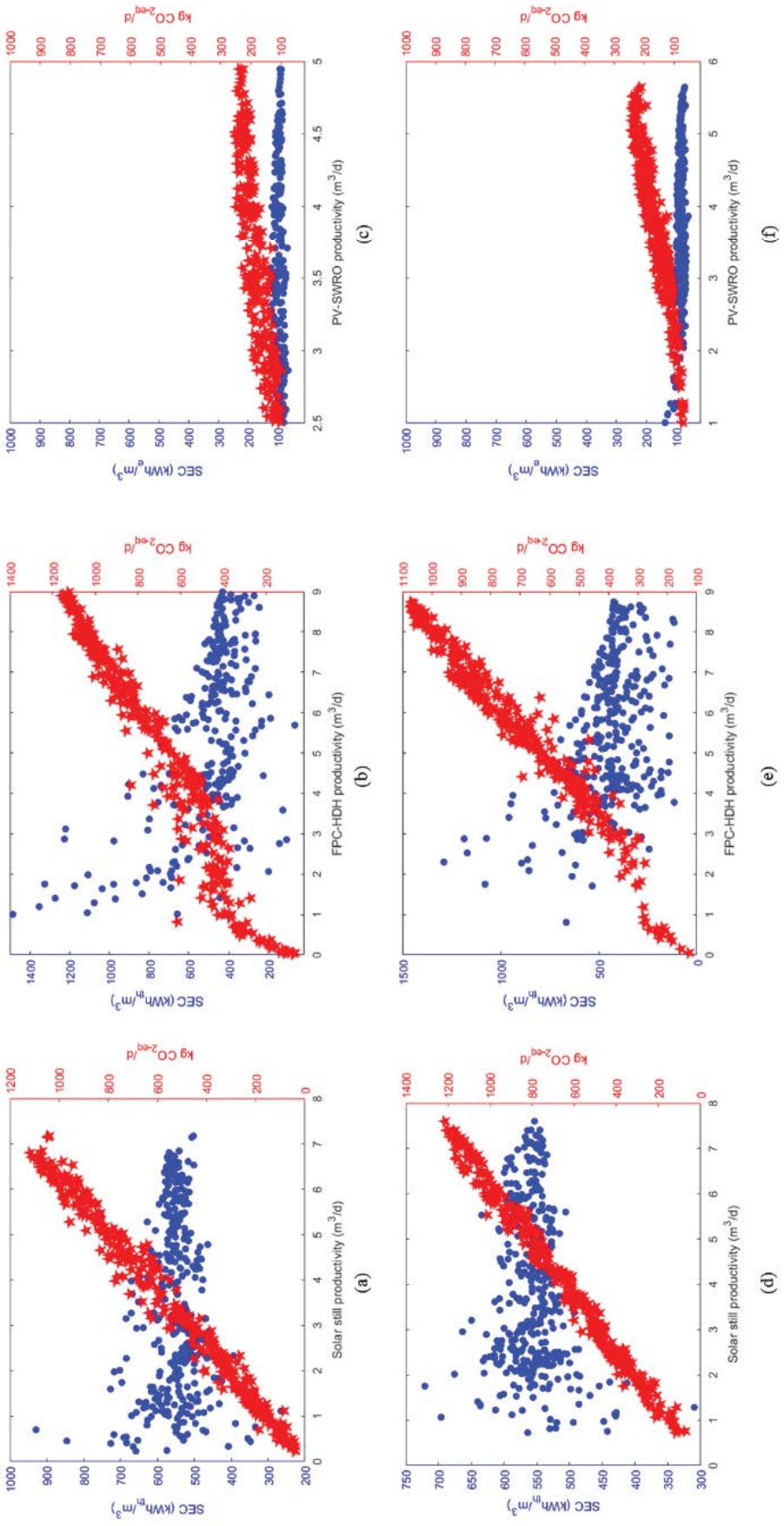

Fig. 6. Specific energy consumption and CO_2-eq emissions mitigated for solar desalination systems in Big Sur and Chañaral.

a linear trend with respect to productivity due to the substitution of using natural gas. Since thermal desalination has higher SEC, the emissions mitigated are high, that is, around 100 to 1200 kg CO_2-eq for 1 to 10 m^3 of daily fresh water productivity, respectively. Since PV-SWRO has a comparatively lower SEC, the emissions mitigated are also lower ranging between 20 and 200 kg CO_2-eq/d. The cumulative total annual emissions avoided are 197.3 ton CO_2-eq and 244.09 ton CO_2-eq for the solar still and FPC-HDH in Big Sur, and around 227.3 ton CO_2-eq and 241.48 ton CO_2-eq in Chañaral, respectively. The annual emissions mitigated for PV-SWRO both locations are about 48.78 and 50.68 ton CO_2-eq, respectively.

4.5. Cost of fresh water

The total direct capital cost for setting up the solar still, FPC-HDH, and PV-SWRO are $87,876, $429,300 and $1,830,269, respectively. The corresponding share of different components is shown in Fig. 7.

It can be seen that, in the case of solar still, the maximum share is by the solar still component materials. Similarly, in the case of FPC-HDH and PV-SWRO system, the predominant share is due to the solar systems, that is, solar collector and solar PV system. In addition, the battery energy storage system in PV-SWRO is also around 19% of the total capital cost. The LCOW for both locations, with higher and lower estimate is shown in Table 5. The high and low values mentioned are the highest LCOW and the lowest LCOW that can be obtained with cost items. In the highest cost case, the solar still, solar collector, and solar PV system costs considered are $500/m^2, $500/m^2 and $2.5/kW with OPEX costs being 20% higher than baseline case. Likewise, in the case of feasible low cost values are with solar still, solar collector and solar PV system costs being $50/m^2, $250/m^2 and $1.75/kW with OPEX costs being 20% lower than baseline case, and CO_2 tax credits availed at $15/ton CO_2 emissions abated annually. With the best combination of cost parameters, it can be seen that the LCOW of freshwater produced by solar stills can be lower than $3/$m^3$ which makes it attractive over other desalination systems for volume of freshwater in this range.

4.6. Sensitivity of cost parameters

Sensitivity analyses of cost components for LCOW of the desalination systems were performed on both locations. The higher and lower values of the CAPEX are for the solar systems, that is, solar still, solar collector and the solar PV system, and are taken according to the literature [41–43]. The OPEX costs vary by 20% of the annual operating cost determined above. In the optimistic case where LCOW is low, the CO_2 tax credits of $ 15/ton of CO_2 emissions abated annually are applied.

Fig. 8 shows the sensitivity analysis for the three desalination systems for both locations. In the case of solar stills, it is observed that the cost of freshwater produced is greatly influenced by the capital cost of the solar still. Likewise, it is found that there is some influence of the discount rate. In the case of FPC-HDH, almost all the parameters, that is, solar collector cost, operational cost, and discount cost influence the LCOW of the freshwater produced. It is also observed that availing CO_2 tax credits is beneficial in reducing the LCOW in the case of these thermal desalination systems. In the case of PV-SWRO system, CAPEX and

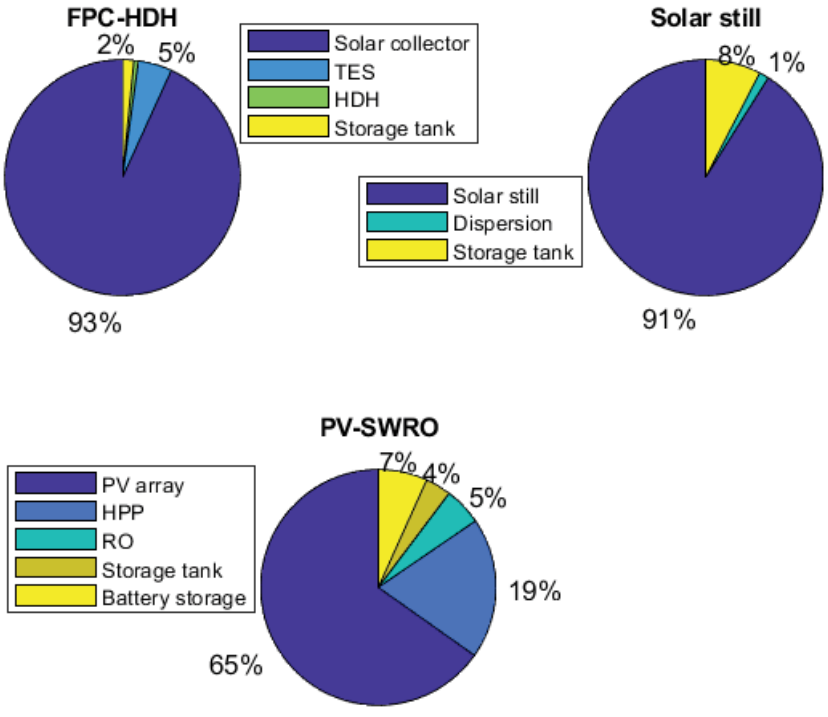

Fig. 7. Share of different items in direct capital costs of solar desalination units.

Table 5
LCOW estimates for desalination of water

LCOW	Big Sur				Chañaral			
	PV-SWRO	Solar still	CSS	FPC-HDH	PV-SWRO	Solar still	CSS	FPC-HDH
Typical ($/m^3)	9.9	8.56	12.88	48.45	8.39	7.59	11.28	40.85
High ($/m^3)	14.33	48.84	78.48	70.8	12.12	43.33	68.77	60.6
Low ($/m^3)	7.22	2.77	4.4	33.07	6.13	2.12	3.32	27.48

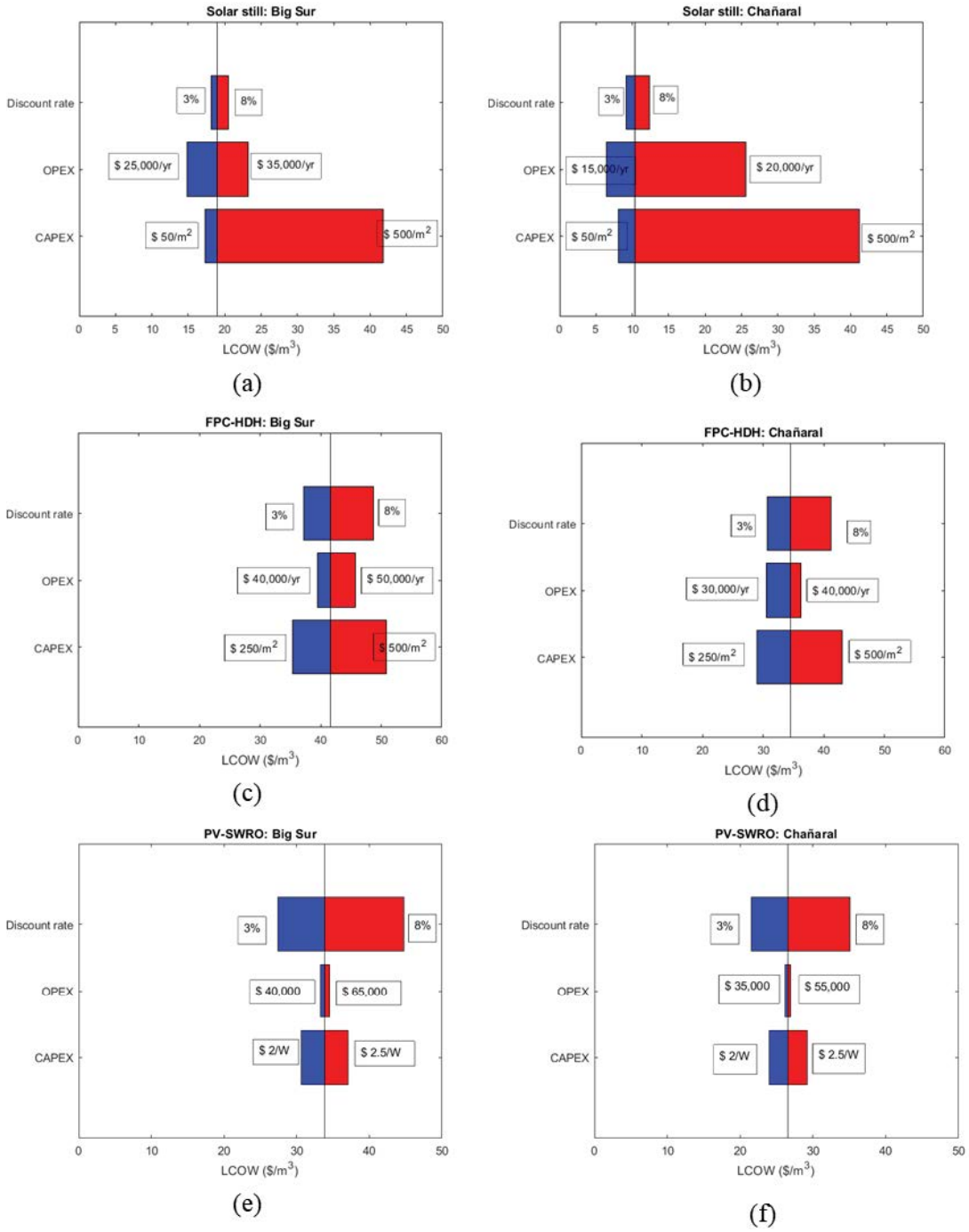

Fig. 8. LCOW sensitivity analysis of desalination systems.

OPEX have some small influence, but the highest influence is observed in the case of the discount rate.

From the analysis performed, all the three systems can produce freshwater in the range greater than 3 m^3/d at costs lower than \$50/m^3, but solar stills might be more advantageous considering that the costs are competitive or lower than the other two systems. The inherent advantage of solar stills is that these are easy to operate, which translates into low annual operational costs.

5. Conclusion

A techno-economic analysis along with environmental assessment of solar stills with inexpensive carbon particles as dispersion was performed and compared two competing solar desalination technologies, that is, solar collector integrated humidification dehumidification (FPC-HDH) system and photo-voltaic seawater reverse osmosis (PV-SWRO) system. Two rural locations: Big Sur (U.S.A) in the northern hemisphere and Chañaral (Chile) in the southern hemisphere were considered. A system energy analysis was performed with real time year-round solar irradiation and ambient conditions data for both locations. It is estimated that the annual freshwater productivity rate of solar stills is only around 3.5 m^3/d for a 1000 m^2 solar still system, while with FPC-HDH, it is around 5 m^3/d. In the case of PV-SWRO, the freshwater productivity with maximum pressure constraint of 55 bar is close to that of the solar still, but incorporating an external storage battery increases the freshwater productivity rate significantly. The estimated annual green-house gas emissions mitigated with thermal desalination system are more than 200 ton of CO_2, while that with PV-SWRO is around 50 tons of CO_2. However, economic analysis showed that solar stills produce freshwater at costs lower than the other two systems. Capital expenditure incurred in installing a solar still system is significantly lower than the other two systems. In addition to this, solar stills being passive are low maintenance systems, and so the annual operational cost is also lower than the other two systems. The FPC-HDH system might not be suitable for low-cost freshwater production, especially since the cost of solar collector is higher. PV-SWRO can also produce freshwater at lower costs, but their complex operational procedure might not be suitable in rural remote regions. With attractive capital cost, operational cost and discount rate, the cost of freshwater produced with a solar still can be lower than \$ 3/m^3, making it a highly feasible option for desalination in remote, rural regions. The analysis carried out constitutes a new approach which allows to evaluate the impact of using low-cost carbon-based nanoparticles in solar stills, assessing the impact of its concentration, and analyzing the effects of increasing the scale of the system. Thus, the analysis, allows also to assess the competitiveness of solar stills, compared to other desalination technologies commonly employed for small communities.

Symbols

A	—	Solar energy incident area, m^2
I	—	Solar irradiance, W/m^2
CAPEX	—	Capital cost, \$
LCOW	—	Levelized cost of water, \$/m^3
m_{hour}	—	Hourly productivity, kg/h
OPEX	—	Annual Operation, maintenance, spares and replacement cost, \$/y
P	—	Saturation pressure, Pa
Q	—	Heat transfer rate, W
R_w	—	Reflectance of water
SEC	—	Specific energy consumption, kWh/m^3
T	—	Temperature, °C
u	—	Wind velocity, m/s
W_p	—	Peak power output, W

Greek

α	—	Absorptance
ρ	—	Emittance
ε	—	HDH effectiveness

Acknowledgements

Significant portion of the work was supported by funding from California Energy Commission contract #GFO-16-503 and USDA NIFA contract #2-15-67021-24117. The authors also express gratitude to Dr. Hugo Pedro (U.C. San Diego) for providing weather data for the location of Big Sur.

References

[1] E. Mathioulakis, V. Belessiotis, E. Delyannis, Desalination by using alternative energy: review and state-of-the-art, Desalination, 203 (2007) 346–365.
[2] WHO, Progress on Household Drinking Water, Sanitation and Hygiene. Special Focus on Inequalities, World Health Organization, 2019.
[3] S. Kalogirou, Seawater desalination using renewable energy sources, Prog. Energy Combust. Sci., 31 (2005) 242–281.
[4] D. Lawal, S. Zubair, M. Antar, Exergo-economic analysis of humidification-dehumidification (HDH) desalination systems driven by heat pump (HP), Desalination, 443 (2018) 11–25.
[5] M. Zubair, A. Al-Sulaiman, M. Antar, S. Al-Dini, N. Ibrahim, Performance and cost assessment of solar driven humidification dehumidification desalination system, Energy Convers. Manage., 132 (2017) 28–39.
[6] M. Darwish, H. Abdulrahim, A. Hassan, A. Mabrouk, PV and CSP solar technologies and desalination: economic analysis, Desal. Water Treat., 57 (2016) 16679–16702.
[7] A. Ghermandi, R. Messalem, Solar-driven desalination with reverse osmosis: the state of the art, Desal. Water Treat., 7 (2009) 285–296.
[8] H. Al-Hinai, M. Al-Nassri, B. Jubran, Effect of climatic, design and operational parameters on the yield of a simple solar still, Energy Convers. Manage., 43 (2002) 1639–1650.
[9] A. Madani, G. Zaki, Yield of solar stills with porous basins, Appl. Energy, 52 (1995) 273–281.
[10] H. Sharon, C. Prabha, R. Vijay, A. Niyas, S. Gorjian, Assessing suitability of commercial fibre reinforced plastic solar still for sustainable potable water production in rural India through detailed energy-exergy-economic analyses and environmnetal impacts, J. Environ. Manage., 295 (2021) 113034, doi: 10.1016/j.jenvman.2021.113034.
[11] A. Tiwari, A. Somwanshi, Techno-economic analysis of mini solar distillation plants integrated with reservoir of garden fountain for hot and dry climate of Jodhpur (India), Sol. Energy, 160 (2018) 216–224.
[12] T. Arunkumar, K. Raj, D. Denkenberger, R. Velraj, Heat carrier nanofluids in solar still – a review, Desal. Water Treat., 130 (2018) 1–16.

[13] S. K. Hota, G. Diaz, Assessment of pyrolytic biochar as a solar absorber material for cost-effective water evaporation enhancement, Environ. Eng. Sci., (2021), doi: 10.1089/ees.2020.0472.
[14] A. Zeiny, H. Jin, G. Lin, P. Song, D. Wen, Solar evaporation via nanofluids: a comparative study, Renewable Energy, 122 (2018) 443–454.
[15] S. Sharshir, G. Peng, L. Wu, N. Yang, F. Essa, A. Elsheikh, S. Mohamed, A. Kabeel, Enhancing the solar still performance using nanofluids and glass cover cooling: experimental study, Appl. Therm. Eng., 113 (2017) 684–693.
[16] T. Elango, A. Kanna, K. Murugavel, Performance study on single basin single slope solar still with different water nanofluids, Desalination, 360 (2015) 45–51.
[17] L. Sahota, S. Arora, H. Singh, S. Sahoo, Thermo-physical characteristics of passive double slope solar still loaded with MWCNTs and Al_2O_3-water based nanofluid, Mater. Today: Proc., 32 (2020) 344–349.
[18] G. Narayan, M. Sharqawy, H. Mostafa, J. Lienhard, S. Zubair, Thermodynamic analysis of humidification dehumidification desalination cycles, Desal. Water Treat., 16 (2010) 339–353.
[19] M. Jones, I. Odeh, M. Haddad, A. Mohammad, J. Quinn, Economic analysis of photovolatic (PV) powered water pumping and desalination without energy storage for agriculture, Desalination, 387 (2016) 35–45.
[20] N. Ahmad, A. Sheikh, P. Gandhidasan, M. Elshafie, Modeling, simulation and performance evaluation of a community scale PVRO water desalination system operated by fixed and tracking PV panels: a case study for Dhahran city, Saudi Arabia, Renewable Energy, 75 (2015) 433–447.
[21] N. Al-Bastaki, A. Abbas, Long-term performance of an industrial water desalination plant, Chem. Eng. Process., 43 (2004) 555–558.
[22] G. Tiwari, S. Shukla, S. Singh, Computer modeling of passive/active solar stills by using inner glass temperature, Desalination, 154 (2003) 171–185.
[23] M. Sharqawy, M. Antar, S. Zubair, A. Elbashir, Optimum thermal design of humidification dehumidification desalination systems, Desalination, 349 (2014) 10–21.
[24] A. Al-Zahrani, A. Orfi, Z. Al-Suhaibani, H. Salim, Al-Ansary, Thermodynamic analysis of a reverse osmosis desalination unit with energy recovery system, Procedia Eng. SWEE2011, 33 (2012) 404–414.
[25] S. Hota, G. Diaz, Activated carbon dispersion as absorber for solar water evaporation: a parametric analysis, Sol. Energy, 184 (2019) 40–51.
[26] S. Hota, G. Diaz, Enhancing solar water evaporation with activated carbon, MRS Adv., (2020) 741–750, doi: 10.1557/adv.2020.267.
[27] S. Kumar, G. Tiwari, Analytical expression for instantaneous exergy efficiency of a shallow basin passive solar still, Int. J. Therm. Sci., 50 (2011) 2543–2549.
[28] A. Robles, V. Duong, A. Martin, J. Guadarrama, G. Diaz, Aluminum minichannel solar water heater performance under year round weather conditions, Sol. Energy, 110 (2014) 356–364.
[29] S. Hota, J. Perez, G. Diaz, Effect of Geometric Configuration and Back Plate Addition in Minichannel Solar Collectors, Conference: ASME 2018 International Mechanical Engineering Congress and Exposition, 2018.
[30] G. Tina, S. Scrofani, Electrical and Thermal Model for PV Module Temperature Evaluation, MELECON 2008 – The 14th IEEE Mediterranean Electrotechnical Conference, IEEE, Ajaccio, France, 2008.
[31] T. Neises, S. Klein, D. Rendl, Development of a thermal model for photovoltaic modules and analysis of NOCT guidelines, J. Sol. Energy Eng., 134 (2011) 01009.
[32] M. Hammami, S. Torretti, F. Grimaccia, G. Grandi, Thermal and performance analysis of a photovoltaic module with an integrated energy storage system, Appl. Sci., 7 (2017) 1107.
[33] S. Lawrence, S. Gupta, G. Tiwari, Experimental validation of thermal analysis of solar still with dye, Int. J. Sol. Energy, 6 (1988) 291–305.
[34] Dupont, Reverse Osmosis Membranes Technical Manual, Dupont Filmtec™, 2020.
[35] J. Miller, J. Lienhard, Impact of extraction on a humidification-dehumidification desalination system, Desalination, 313 (2013) 87–96.
[36] W. Soto, S. Klein, W. Beckman, Improvmeent and validation of a model for photovoltaic array performance, Sol. Energy, 80 (2006) 78–88.
[37] Y.-Y. Lu, Y.-D. Hu, X.-L. Zhang, L.-Y. Wu, Q.-Z. Liu, Optimum design of reverse osmosis system under different feed concentration and product specification, J. Membr. Sci., 287 (2007) 219–229.
[38] R. Semiat, Energy issues in desalination processes, Environ. Sci. Technol., 42 (2008) 8193–8201.
[39] M. Alhaj, G. Al-Ghamdi, Why is powering thermal desalination with concentrated solar power expensive? Assessing economic feasibility and market commercialization barriers, Sol. Energy, 189 (2019) 480–490.
[40] S. Karki, K. Haapala, B. Fronk, Technical and economic feasibility of solar flat-plate collector thermal energy systems for small and medium manufacturers, Appl. Energy, 254 (2019) 113649.
[41] D. Trier, C. Skov, S. SØrensen, F. Bava, Solar District Heating Trends and Possibilities – Characteristics of Ground-Mounted Systems for Screening of Land Use Requirements and Feasibility, SHC: Solar Heat and Energy in Urban Environments, 2018.
[42] Z. Tian, B. Perers, S. Furbo, J. Fan, Thermo-economic optimization of a hybrid solar disctirct heating plant with flat plate collectors and parabolic trough collectors in series, Energy Convers. Manage., 165 (2018) 92–101.
[43] D. Feldman, R. Margolis, Q2/Q3 2020 Solar Industry Update, NREL, 2020.
[44] A. Malek, M. Hawlader, J. Ho, Design and economics of RO seawater desalination, Desalination, 105 (1996) 245–261.
[45] A. Zurita, C. Mata-Torres, C. Valenzuela, C. Felbol, J. Cardemil, A. Guzman, R. Escobar, Techno-economic evaluation of a hybrid CSP+PV plant integrated with thermal energy storage and a large-scale battery energy storage system for base generations, Sol. Energy, 173 (2018) 1262–1277.
[46] M. Ashby, Appendix-A. Data for Engineering Materials, in Materials Selection in Mechanical Design (4th ed.), Butterworth-Heinemann, Oxford, 2011, pp. 495–523.
[47] H. El-Dessouky, H. Ettouney, Chapter 10 – Economic Analysis of Desalination Processes, In: Fundamentals of Salt Water Desalination, Elsevier Science, 2002, pp. 503–524.
[48] K. Thomas, Overview of Village Scale, Renewable Energy Powered Desalination, NREL, 1997.
[49] B. Widyolar, L. Jiang, J. Brinkley, S. Hota, J. Ferry, G. Diaz, R. Winston, Experimental performance of an ultra-low-cost solar photovoltaic-thermal (PVT) collector using aluminum minichannels and nonimaging optics, Appl. Energy, 268 (2020) 114894.
[50] M. Gumustas, C. Sengel-Turk, A. Gumustas, S. Ozkan, B. Uslu, Chapter 5 – Effect of Polymer-Based Nanoparticles on the Assay of Antimicrobial Drug Delivery Systems, In: Multifunctional Systems for Combined Delivery, Biosensing and Diagnostics, Elsevier, 2017, pp. 67–108.
[51] M. Gupta, V. Singh, R. Kumar, Z. Said, A review on thermophysical properties of nanofluids and heat transfer applications, Renewable Sustainable Energy Rev., 74 (2017) 638–670.